Journal of Power Sources 262 (2014) 239–244

Contents lists available at ScienceDirect

Journal of Power Sources

journal homepage: www.elsevier.com/locate/jpowsour

Influences of $Gd_2Ti_2O_7$ sintering aid on the densification, ionic conductivity and thermal expansion of $Gd_{0.1}Ce_{0.9}O_{1.95}$ electrolyte for solid oxide fuel cells

Ting Guo, Lei Zhang, Xiao Song, Xiaolei Dong, Mandar M. Shirolkar, Meng Wang, Ming Li, Haiqian Wang*

Hefei National Laboratory for Physical Sciences at Microscale, University of Science and Technology of China, 96 Jinzhai Road, Hefei, Anhui 230026, PR China

HIGHLIGHTS

- $Gd_2Ti_2O_7$ is an effective sintering aid for GDC.
- The relative density of $Gd_2Ti_2O_7$-added GDC can reach over 97% by sintering at 1400 °C for 5 h.
- The ionic conductivity decrease of the $Gd_2Ti_2O_7$-added GDC is small.
- The thermal expansion coefficient of GDC can be reduced by adding $Gd_2Ti_2O_7$.
- $Gd_2Ti_2O_7$ is chemically stable and does not react with GDC.

ARTICLE INFO

Article history:
Received 7 January 2014
Received in revised form
16 March 2014
Accepted 18 March 2014
Available online 26 March 2014

Keywords:
Gadolinium titanate
Gadolinium-doped ceria
Sintering aid
Densification
Ionic conductivity
Thermal expansion coefficient

ABSTRACT

The effects of $Gd_2Ti_2O_7$ (GT) as sintering aid on the densification, electrical properties and thermal expansion of $Gd_{0.1}Ce_{0.9}O_{1.95}$ (GDC) are examined. Samples added with TiO_2 sintering aid are also tested for comparison. It is found that by sintering at a moderate temperature of 1400 °C for 5 h, the relative density of the GT-added GDC can reach over 97% as the molar ratio of GT/GDC reaches 0.02 or higher. XRD analysis indicates that GT does not react with GDC, while TiO_2 reacts with Gd in GDC to form GT. The ionic conductivities of the GT-added and the TiO_2-added GDC are analyzed by AC impedance spectroscopy at 500–700 °C. The result shows that although the ionic conductivity of the GT-added GDC decreases as the GT/GDC molar ratio increases up to 0.05, it is still higher than that of 8YSZ and much higher than that of the GDC added with an equivalent amount of TiO_2. It is also found that the thermal expansion coefficient of GDC decreases as the amount of GT increases. These results show that GT is an excellent sintering aid for GDC, and the optimal molar ratio of GT/GDC is 0.02 in terms of densification and ionic conductivity.

1. Introduction

Solid electrolytes exhibiting high oxygen ionic conductivity in the low temperature range are of special interest for their application in the solid oxide fuel cells [1]. Gd-doped CeO_2 (GDC, $Gd_xCe_{1-x}O_{2-2/x}$, $0.1 \leq x \leq 0.25$) exhibits much higher ionic conductivity between 500 and 700 °C as compared to zirconia based electrolytes [2–4]. Therefore, GDC is considered as one of the most promising solid electrolytes for SOFCs working below 700 °C.

However, GDC has a very high melting temperature (about 2300 °C [5]) and the refractory nature of GDC leads to significant challenges in its application in SOFCs. Since the electrolyte materials are usually co-sintered with other cell components, lower sintering temperature (≤1400 °C) is desired to the restrain solid state reactions, diffusions between ceramic materials and to avoid other serious problems [4,6]. Hence, various efforts have been made to reduce the sintering temperature of GDC by the addition of sintering aids such as CoO, MnO_2, Bi_2O_3 and Li_2O [7–10]. Specifically, TiO_2 is also explored as a sintering aid for ceria based materials, since Chen et al. found that TiO_2 addition in CeO_2 enhances the grain boundary mobility during sintering [11]. For example, Culter et al. have shown that 1 mol% addition of TiO_2 obviously increases the sintering activity of $Ce_{0.8}Sm_{0.2}O_{1.9}$ electrolyte [12]. Ge

* Corresponding author. Tel.: +86 551 63603770; fax: +86 551 63606266.
E-mail addresses: hqwang@ustc.edu.cn, yhgong@mail.ustc.edu.cn (H. Wang).

http://dx.doi.org/10.1016/j.jpowsour.2014.03.077
0378-7753/

et al. introduced TiO_2 as the sintering aid for $Gd_{0.2}Ce_{0.8}O_{1.9}$ and observed that the sintering temperature can be lowered from 1600 °C to 1400 °C [13]. Pikalova et al. optimized the composition of $(1-x)Ce_{0.8}Gd_{0.2}O_{1.9} + xTiO_2$ ($x = 0.01$–0.06) both in the air and hydrogen atmosphere, and found that the optimal content of TiO_2 is 2 mol% from the viewpoint of sintering and electrical properties [14].

However, TiO_2 reacts with the Gd from GDC to form $Gd_2Ti_2O_7$ (GT) and thus changes the composition of GDC [14], which is not expected. Therefore, it is essential to explore an appropriate sintering aid material which does not react with GDC. GT can be regarded as a reaction product of Gd_2O_3 and TiO_2. It is stoichiometric and has a stable pyrochlore phase. Thus, the reaction between GT and GDC can be effectively suppressed. Moreover, the melting point of GT (≈1820 °C) is much lower than that of GDC [15]. In general, the sintering temperature of ceramics can be reduced by utilizing the sintering aids with a low melting temperature, even if the melting point of sintering aid is higher than the sintering temperature. For example, Al_2O_3 (melting point ≈ 2050 °C) can be well sintered at 1550 °C with MnO (melting point ≈ 1785 °C) as the sintering aid, because an eutectic composition is formed at 1520 °C [16].

In this work, we have introduced GT, which can significantly enhance the sintering behaviors of $Gd_{0.1}Ce_{0.9}O_{1.95}$ without changing its composition obviously. Meanwhile, the ionic conductivity of the GT-added GDC decreases within the acceptable range. In addition, the thermal expansion coefficient (TEC) of GDC is reduced after GT is added.

2. Experimental

2.1. Sample preparation

All the precursor chemicals used are of analytical grade (purity ≈ 99.9%) and used as received without further purification. To obtain GT powder, TiO_2 (Runyu Chemical, China) and Gd_2O_3 (Ourchem, China) powders were mixed in a molar ratio of 2:1 and ball milled for 2 h followed by sintering at 1400 °C for 2 h. The obtained powder was ball milled again for another 2 h. GT powder shown in Fig. 1 exhibits non-uniform particle size which spans from about 100 nm to 2.5 μm. The different GT-added GDC samples were obtained by grinding the GT powder with $Gd_{0.1}Ce_{0.9}O_{1.95}$ (average particle size is 80 nm, Nextech, USA). For the comparison, TiO_2-added GDC samples were also prepared with the same grinding method. Then the samples in the pellet form were prepared by pressing the powders under a pressure of about 200 MPa and sintering in air at 1400 °C for 5 h. The sintered pellets were approximately 11 mm in diameter and 1 mm in thickness. The sample IDs corresponding to the GT-added and TiO_2-added GDC are listed in Table 1.

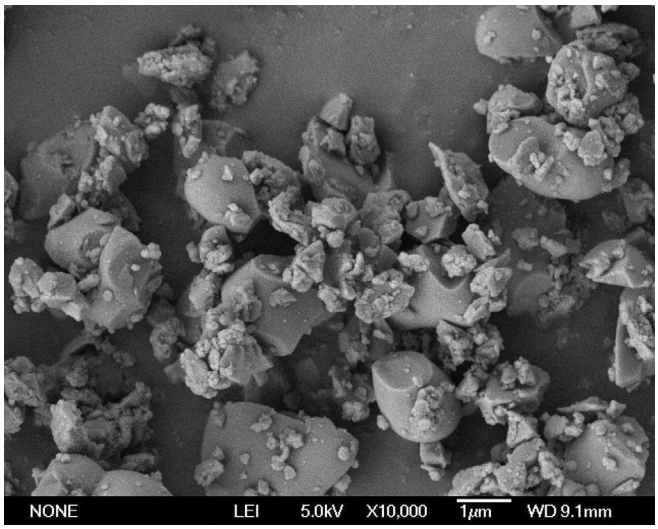

Fig. 1. SEM image of the microstructure of GT starting powder.

2.2. Measurement

The density of the GT-added GDC pellet samples was measured by Archimedes method. The microstructure of the samples was obtained by scanning electron microscopy (SEM, JSM6700, JOEL). SEM-based (SIRION200, FEI) energy dispersive X-ray spectroscopy (EDS) and electron backscatter diffraction (EBSD) were used to examine the elemental distribution of the samples. The phase of the samples (grounded into powders) was evaluated by an X-ray diffractometer (XRD, MXPAHF, MacScience) with Cu Kα radiation over the range of $2\theta = 20°$–$80°$ at room temperature. The thermal expansion measurements were conducted with Netzsch DIL 402C dilatometer in the air. The electrical properties were measured by an electrochemical workstation (IM6eX, Zahner) from 500 to 700 °C with two probe method. In order to obtain good electrical contacts, Ag paste was applied on both the sides of the pellets and dried at 120 °C for 2 h before the electrical measurements. The AC impedance spectra were measured in the air over 0.1 Hz–1 MHz frequency range with 20 mV of AC signal amplitude from 500 to 700 °C.

3. Results and discussion

3.1. XRD analysis

The XRD patterns of GDC, GT-added GDC (0.5GT, 2GT, 5GT) and TiO_2-added GDC (10T) samples are shown in Fig. 2. Here, we have selected the sample 10T for the comparison because theoretically, the amount of Gd in GDC and Ti in TiO_2 are stoichiometric for the reaction to form GT. For the GT-added GDC, GT related XRD peaks can be observed when the GT/GDC molar ratio is above 0.02, and no peaks of any other phases were observed. From the inset of Fig. 2, it can be seen that the (111) peak of the GT-added GDC hardly shifts (less than 0.01°), suggesting that GDC almost keeps the original composition even after GT is added. On the other hand, for the 10T sample, along with GDC phase a secondary phase was observed. The phase was identified as GT with pyrochlore structure. The pattern also shows the absence of peaks related to TiO_2, indicating that TiO_2 reacts with Gd in GDC to form GT phase. As we know that the ionic radius of Gd^{3+} (0.119 nm) is larger than that of Ce^{4+} (0.111 nm) [17], thus the lattice constant of GDC decreases as the content of Gd^{3+} decreases [18]. It can be seen from the inset of Fig. 2 that the (111) peak of 10T sample shift to a higher angle nearly by 0.03° as compared to that of GDC. The calculated lattice constants of the GDC and 10T samples are $a = 5.417$ Å and 5.412 Å respectively. It can be seen that the lattice constant of 10T sample coincides with the lattice constant reported for the undoped CeO_2 ($a = 5.412$ Å,

Table 1
The sample IDs corresponding to GDC added with different amount of GT or TiO_2.

Sample ID	GT/GDC mol ratio	Sample ID	TiO_2/GDC mol ratio
GDC	0		
0.5GT	0.005	1T	0.01
2GT	0.02	4T	0.04
5GT	0.05	10T	0.10

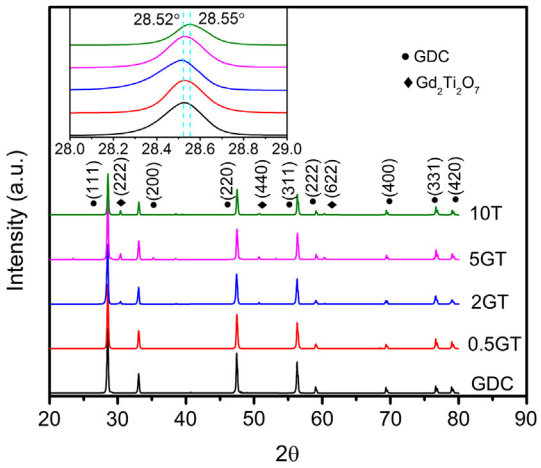

Fig. 2. XRD patterns of GDC, 0.5GT, 2GT, 5GT and 10T powders sintered at 1400 °C for 5 h.

2003 JCPDS database, #81-0792), implying that nearly all Gd^{3+} in GDC is reacted with TiO_2 in the 10T sample.

3.2. Densification

3.2.1. Relative density

The relative density of different GT-added GDC is shown in Fig. 3. It is found that the relative density of GDC increases as the ratio of GT/GDC increases. Interestingly, for the sample 2GT, the relative density reaches as high as 97%, which is dense enough to meet the generally acceptable density criteria (≥95%) [19] for SOFC electrolyte. As the GT/GDC ratio further increases, the improvement in the densification of GDC is not so obvious because the relative density is already very high.

3.2.2. Microstructure and sintering behavior

Fig. 4 shows the microstructure of different GT-added GDC. It is clearly seen that the grain size increases from 1 to 2 μm for pure GDC to 6–7 μm for 5GT samples. Meanwhile, the pores on the surface of GDC decrease obviously as the amount of GT increases. When the GT/GDC molar ratio reaches 0.02 (i.e. sample 2GT), the sample is already very dense (see Fig. 3), hence nearly no pores can be seen in the 2GT and 5GT samples.

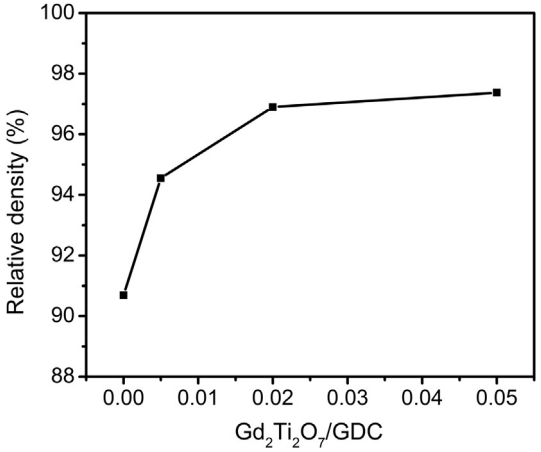

Fig. 3. The relative density of different GT-added GDC.

In order to better understand the sintering process, SEM, EBSD and EDS analyses were taken on the sample 5GT and presented in Fig. 5. As indicated by EDS spectroscopy, the dark gray grains in Fig. 5b (e.g., area A) can be assigned to GT and the light gray grains (e.g., area B) can be assigned to GDC. It is seen that the edges of the GT grains become round and blunt after sintered at 1400 °C, as compared to those before sintering (see Fig. 1). This implies that the GT grains or at least the GT grain boundaries, have gone through a melting process during sintering. The GDC grain sizes in the areas without GT aggregation are much larger than those in Fig. 4a, which indicates that the GDC grains are effectively sintered with the help of GT sintering aid, even though we cannot see apparent GT grains in such areas. So, we think that GT with a limited solubility in GDC, tends to reside in the GDC grain boundaries and form a thin grain boundary layer. The ionic conductivity analysis discussed in the next section also supports the formation of a thin grain boundary layer. Such a grain boundary layer enhances the grain boundary diffusion and promotes the grain growth. Gauckler et al. studied the sintering behavior of cobalt oxide doped GDC, and suggested that the improved sintering properties could be assigned to a grain boundary film acting as a short circuit path for mass transportation across the GDC grain boundaries [20].

On the other hand, in the GT aggregated areas, the GDC grains are smaller, and the shape of the GDC grains may be slender and concave (see area C in Fig. 5b). Such small and irregular grains are unfavorable for lowering the surface energy of the grains. This is due to the fact that the insoluble GT grains inhibit the grain boundary migration and suppress the grain growth. The above discussions also suggest that better sintering behaviors can be expected by using smaller and uniformly distributed GT particles.

3.3. Ionic conductivity

To investigate the effects of GT addition on the electrical properties of GDC, the samples were analyzed by AC impedance spectroscopy. The electrical properties of TiO_2-added GDC are also investigated for comparison. Fig. 6 shows typical impedance spectra of samples tested at 600 °C in the air. Here, the impedance spectra are obtained by subtracting the leads/instrument impedance from the measured data. It is reported that by using this method, the high frequency arc, which corresponding to the grain boundary resistance, could be more accurately determined, especially at high temperatures [21]. In general, the AC impedance of an ionic conductor measured by the two-probe method contains the contributions from grain interior (bulk), grain boundary, and electrode–electrolyte interface polarization [22]. The total resistance (R_T) of the electrolyte can be given by the equation:

$$R_T = R_{gi} + R_{gb} \quad (1)$$

where R_{gi} and R_{gb} are the grain interior (bulk) resistance and the grain boundary resistance, respectively. The conductivity value (σ) can be obtained by:

$$\sigma = \frac{L}{R_T \cdot S} \quad (2)$$

where L and S represent the sample thickness and electrode area of the sample, respectively.

The obtained grain interior resistance and grain boundary resistance for different samples at 600 °C are listed in Table 2. It is seen that for the GT-added samples, the grain interior resistance does not increase much, while the grain boundary resistance increases a lot as the GT content grows, suggesting that GT, which exhibits low ionic conductivity (less than 1.1×10^{-5} S cm^{-1} at

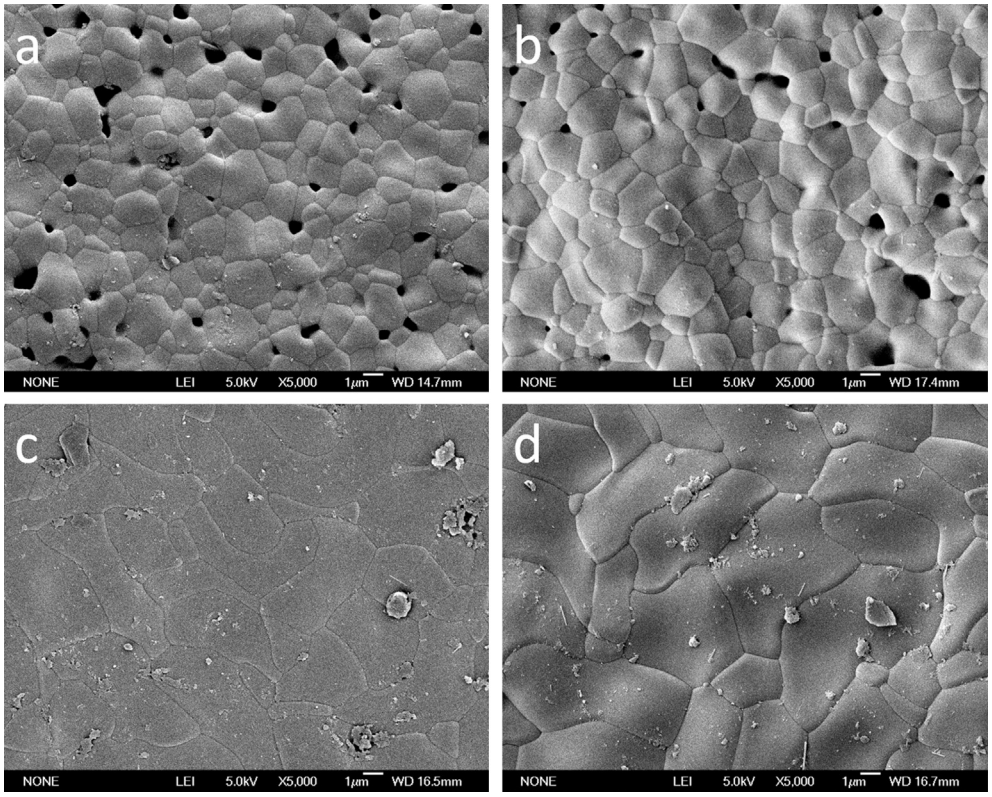

Fig. 4. SEM images of the surface of (a) GDC, (b) 0.5GT, (c) 2GT, (d) 5GT sintered at 1400 °C for 5 h.

600 °C [23–25]), is mainly distributed in the grain boundaries. This is consistent with the discussions regarding the EBSD and EDS results. While, as for the TiO_2-added samples, the grain interior resistance and the grain boundary resistance changes are similar to those of the GT-added samples, except that the grain boundary resistance increases much more rapidly. This is probably due to the fact that the reaction between Gd^{3+} and TiO_2 is prone to take place in the grain boundary region. As we know, the extraction of Gd by the TiO_2 will lead to formation of pure CeO_2, which has a very low ionic conductivity [26].

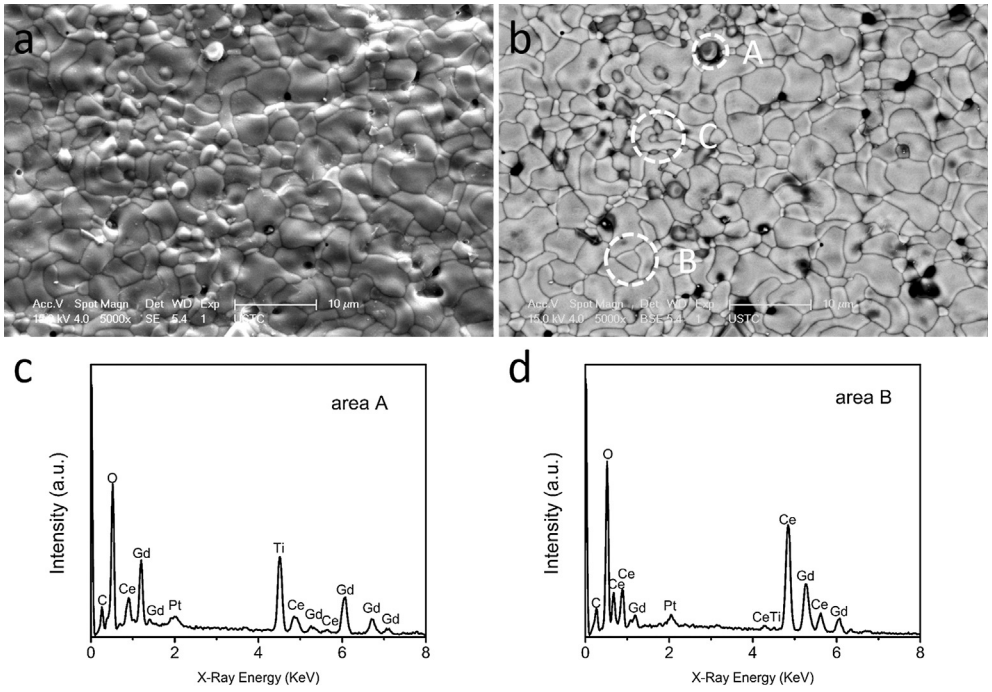

Fig. 5. SEM image and the corresponding EBSD image with EDS analysis of the surface of 5GT: (a) SEM image; (b) EBSD image; (c) EDS analysis of area A; (d) EDS analysis of area B.

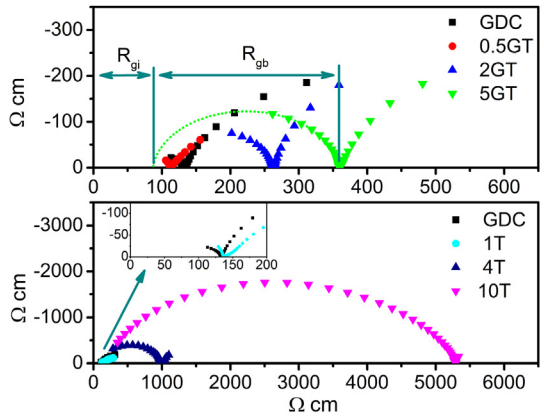

Fig. 6. Nyquist diagram of the impedance spectra for GT-added and TiO_2-added GDC at 600 °C in the air.

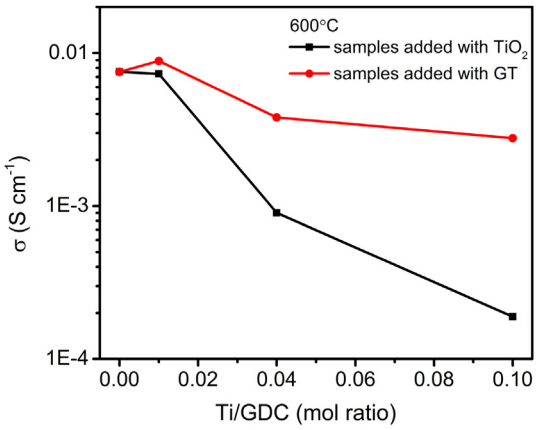

Fig. 7. The ionic conductivity of GT-added and TiO_2-added GDC as a function of Ti/GDC ratio at 600 °C in the air.

The calculated total ionic conductivity of different samples at 600 °C is shown in Fig. 7. It is observed that the ionic conductivity decreases from 7.52×10^{-3} to 2.78×10^{-3} S cm^{-1} as GT/GDC ratio increases from 0 to 0.05. It is also a point of interest to see that the ionic conductivity of the sample 0.5GT is even a little higher than that of GDC, which may be attributed to the increase in the relative density due to the addition of the GT. On the other hand, it also indicates that the ionic conductivity of GDC is negligibly affected by the presence of a small amount of GT. While, for the TiO_2-added samples, the ionic conductivity decreases quickly from 7.52×10^{-3} to 1.89×10^{-4} S cm^{-1} as TiO_2/GDC ratio increases from 0 to 0.10. We can see that although the ionic conductivities of the GT-added samples decrease, they are still much better than those of the samples added with an equivalent amount of TiO_2. Here, the ionic conductivity deterioration of TiO_2-added GDC is much more serious than that reported in literature [13,14], which may be attributed to the different Gd amount in the $Gd_{0.1}Ce_{0.9}O_{1.95}$ (GDC10, used in our experiment) and $Gd_{0.2}Ce_{0.8}O_{1.9}$ (GDC20, used in Refs. [13,14]). As we know, the ionic conductivity of $Gd_xCe_{1-x}O_{2-2/x}$ is high when x is in the range of 0.1 to 0.25, but it falls quickly when x exceeds this range [2–4]. In the case of GDC10, the extraction of Gd by TiO_2 makes the x less than 0.1 and results in serious ionic conductivity loss. However, in the case of GDC20, partial loss of Gd still makes the x in a suitable range, and thus may have little effect or even a positive effect on the ionic conductivity (some reports have shown that GDC10 has a higher ionic conductivity than GDC20 [27,28]). As a summary, the presence of a low concentration of GT may not have a dominant effect on deteriorating the conductivity, but the excess extraction of Gd from GDC by TiO_2 is fatal to the ionic conduction.

Fig. 8 shows the Arrhenius plots of the ionic conductivities of the samples in the temperature range between 500 and 700 °C. The calculated activation energy of different samples is listed in Table 3. The result shows that the activation energy increases slightly as the concentration of GT grows, while it increases rapidly as the concentration of TiO_2 grows. Meanwhile, it is found that although the ionic conductivity of GDC may decrease after GT is added, all the samples added with GT have higher ionic conductivities than 8YSZ [29], a widely used electrolyte material. This means the GT-added GDC is still suitable for the electrolyte material of SOFC. By contrast, the ionic conductivity of the TiO_2-added GDC decreases rapidly with the increasing amount of TiO_2. For example, the 4T sample, which has an equivalent Ti amount compared to 2GT sample, already has a much lower ionic conductivity than 8YSZ. This indicates that GT is a better sintering aid for GDC as compared to TiO_2.

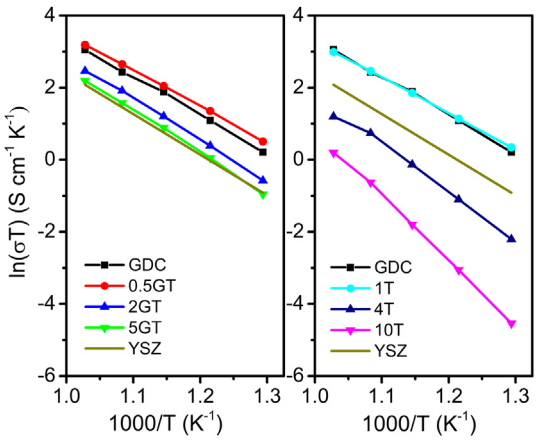

Fig. 8. Arrhenius plot of GDC with different GT and TiO_2 contents.

3.4. Thermal expansion

The thermal expansion property of the different GT-added GDC is also investigated and shown in Fig. 9. The average TEC data of

Table 2
The grain interior resistance and grain boundary resistance of GDC added with different amount of GT or TiO_2.

Sample ID	Grain interior resistance (Ω cm)	Grain boundary resistance (Ω cm)
GDC	68	65
0.5GT	59	54
2GT	81	181
5GT	89	271
1T	63	74
4T	85	916
10T	101	5196

Table 3
The activation energy of GDC added with different amount of GT or TiO_2.

Sample ID	Activation energy (eV)	Sample ID	Activation energy (eV)
GDC	0.91		
0.5GT	0.87	1T	0.86
2GT	0.99	4T	1.13
5GT	1.02	10T	1.55

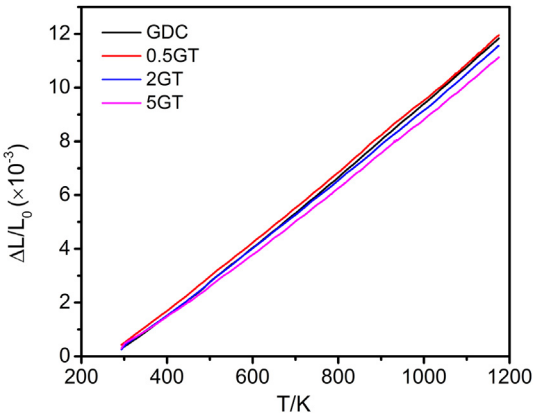

Fig. 9. Dilatometric data of different GT-added GDC as a function of temperature.

Table 4
The average TECs of different GT-added GDC between 293 and 1173 K.

Sample ID	GT/GDC mol ratio	Average TEC (10^{-6} K^{-1})
GDC	0	13.08
0.5GT	0.005	13.06
2GT	0.02	12.82
5GT	0.05	12.28

different GT-added GDC in the temperature range of 293 and 1173 K is calculated and listed in Table 4. It is found that the TEC decreases from 13.08 $\times$ 10^{-6} to 12.28 $\times$ 10^{-6} K^{-1} as the molar ratio of GT/GDC increases from 0 to 0.05. This is mainly due to the fact that GT has a low TEC (10.82 $\times$ 10^{-6} K^{-1} at 1523 K) [30] which is comparable to YSZ ($\sim$10–11 $\times$ 10^{-6} K^{-1} at 1473 K) [31].

It is known that GDC is prone to reduction at low oxygen partial pressures [32], which gives rise to electronic conduction and thus, results in a non-negligible loss in the open-circuit voltage (OCV) of the cell. Moreover, the lattice expansion of the ceria electrolyte at the fuel side caused by GDC reduction will lead to mechanical stability problems [33,34]. One approach to overcome this problem is to coat GDC with a very thin YSZ film to form a bilayer electrolyte [35,36], but the thermal expansion mismatch between GDC and YSZ can be a main difficulty in this situation [37]. According to the TEC result, GT can be used to adjust the TEC of GDC to improve the thermal expansion matching properties of YSZ–GDC dual-layer electrolyte. However, considering that the ionic conductivity also decreases as the GT content increases, there is a trade-off between the TEC and the ionic conductivity when selecting the ratio of GT/GDC.

4. Conclusions

In the present work, the effects of GT as a sintering aid on the densification, electrical properties and thermal expansion of GDC are examined. Samples added with TiO_2 sintering aid are also tested for comparison. It is found that by sintering at a moderate temperature of 1400 °C for 5 h, the relative density of the GT-added GDC can reach over 97% as the molar ratio of GT/GDC reaches 0.02 or higher. XRD analysis indicates that GDC almost keeps its original composition after GT is added, while TiO_2 reacts with Gd in GDC to form GT. The AC impedance analysis result shows that although the ionic conductivity of the GDC decreases as GT/GDC molar ratio increases up to 0.05, it is still higher than that of 8YSZ and much higher than that of the GDC added with an equivalent amount of TiO_2. It is also found that the thermal expansion coefficient of GDC decreases as the amount of GT increases. These results indicate that GT is an excellent sintering aid for GDC. Overall, the optimal molar ratio of GT/GDC is 0.02 for the reason that 2GT has a high relative density and a relatively high ionic conductivity.

References

[1] T. Hibino, A. Hashimoto, T. Inoue, J. Tokuno, S. Yoshida, M. Sano, Science 288 (2000) 2031–2033.
[2] T.S. Zhang, P. Hing, H.T. Huang, J. Kilner, Solid State Ionics 148 (2002) 567–573.
[3] X.B. Li, Z.J. Feng, J.S. Lu, F.J. Wang, M.S. Xue, G.Q. Shao, Ceram. Int. 38 (2012) 3203–3207.
[4] L. Gao, M. Zhou, Y.F. Zheng, H.T. Gu, H. Chen, L.C. Guo, J. Power Sources 195 (2010) 3130–3134.
[5] M.A. Kovalenko, A.Y. Kupryazhkin, J. Nucl. Mater. 430 (2012) 12–19.
[6] T.S. Zhang, J. Ma, H.T. Huang, P. Hing, Z.T. Xia, S.H. Chan, J.A. Kilner, Solid State Sci. 5 (2003) 1505–1511.
[7] T.S. Zhang, J. Ma, L.B. Kong, S.H. Chan, P. Hing, J.A. Kilner, Solid State Ionics 167 (2004) 203–207.
[8] A.K. Baral, H.P. Dasari, B.K. Kim, J.H. Lee, J. Alloy Compd. 575 (2013) 455–460.
[9] V. Gil, J. Tartaj, C. Moure, P. Duran, Ceram. Int. 33 (2007) 471–475.
[10] J.D. Nicholas, L.C. De Jonghe, Solid State Ionics 178 (2007) 1187–1194.
[11] P.L. Chen, I.W. Chen, J. Am. Ceram. Soc. 79 (1996) 1793–1800.
[12] R.A. Cutler, D.L. Meixner, B.T. Henderson, K.N. Hutchings, D.M. Taylor, M.A. Wilson, Solid State Ionics 176 (2005) 2589–2598.
[13] L. Ge, R.F. Li, S.C. He, H. Chen, L.C. Guo, Int. J. Hydrogen Energy 37 (2012) 16123–16129.
[14] E.Y. Pikalova, V.I. Maragou, A.K. Demin, A.A. Murashkina, P.E. Tsiakaras, Solid State Ionics 179 (2008) 1557–1561.
[15] J.L. Waring, Sj Schneide, J. Res. Natl. Bur. Stand. A69 (1965) 255.
[16] M. Sathiyakumar, F.D. Gnanam, Ceram. Int. 28 (2002) 195–200.
[17] R.D. Shannon, Acta Crystallogr. A 32 (1976) 751–767.
[18] K. Singh, S.A. Acharya, S.S. Bhoga, Ionics 12 (2006) 295–301.
[19] N.Q. Minh, J. Am. Ceram. Soc. 76 (1993) 563–588.
[20] E. Jud, L.J. Gauckler, J. Electroceram. 14 (2005) 247–253.
[21] L. Zhang, F. Liu, K. Brinkman, K.L. Reifsnider, A.V. Virkar, J. Power Sources 247 (2014) 947–960.
[22] B.S. Prakash, V.K.W. Grips, S.T. Aruna, J. Power Sources 214 (2012) 358–364.
[23] A.V. Shlyakhtina, O.K. Karyagina, L.G. Shcherbakova, Inorg. Mater. 40 (2004) 59–65.
[24] S.A. Kramers, H.L. Tuller, Solid State Ionics 82 (1995) 15–23.
[25] M. Mori, G.M. Tompsett, N.M. Sammes, E. Suda, Y. Takeda, Solid State Ionics 158 (2003) 79–90.
[26] M.A. Panhans, R.N. Blumenthal, Solid State Ionics 60 (1993) 279–298.
[27] B.C.H. Steele, Solid State Ionics 129 (2000) 95–110.
[28] K.C. Anjaneya, G.P. Nayaka, J. Manjanna, G. Govindaraj, K.N. Ganesha, J. Alloy Compd. 578 (2013) 53–59.
[29] S. Ikeda, O. Sakurai, K. Uematsu, N. Mizutani, M. Kato, J. Mater. Sci. 20 (1985) 4593–4600.
[30] Z.G. Liu, J.H. Ouyang, Y. Zhou, X.L. Xia, Mater. Des. 30 (2009) 3784–3788.
[31] A.G. Evans, M.Y. He, J.W. Hutchinson, Prog. Mater. Sci. 46 (2001) 249–271.
[32] M. Mogensen, N.M. Sammes, G.A. Tompsett, Solid State Ionics 129 (2000) 63–94.
[33] A. Atkinson, Solid State Ionics 95 (1997) 249–258.
[34] S.P.S. Badwal, F.T. Ciacchi, J. Drennan, Solid State Ionics 121 (1999) 253–262.
[35] Q.L. Liu, K.A. Khor, S.H. Chan, X.J. Chen, J. Power Sources 162 (2006) 1036–1042.
[36] A. Tsoga, A. Gupta, A. Naoumidis, D. Skarmoutsos, P. Nikolopoulos, Ionics 4 (1998) 234–240.
[37] T. Horita, N. Sakai, H. Yokokawa, M. Dokiya, T. Kawada, J. Van Herle, K. Sasaki, J. Electroceram. 1 (1997) 155–164.